HOKKAIDO UNIVERSITY

Title	Extension of Dowell and Semi-Analytical Homogenization Methods for Time-Domain Analysis of Magnetic Devices
Author(s)	五十嵐, 一; リウ, チャオ; Shuli, Yin
Citation	IEEE Transactions on Magnetics, 61(1), 1-9 https://doi.org/10.1109/tmag.2024.3498010
Issue Date	2024-11-14
Doc URL	https://hdl.handle.net/2115/99256
Rights	© 2025 IEEE. Personal use of this material is permitted. Permission from IEEE must be obtained for all other uses, in any current or future media, including reprinting/republishing this material for advertising or promotional purposes, creating new collective works, for resale or redistribution to servers or lists, or reuse of any copyrighted component of this work in other works.
Type	journal article
File Information	igarashi-magnetics-HUSCAP2024.pdf

Hokkaido University Collection of Scholarly and Academic Papers : HUSCAP

Extension of Dowell and Semi-Analytical Homogenization Methods for Time-domain Analysis of Magnetic Devices

Hajime Igarashi, *Member*, *IEEE*, Qiao Liu and Shuli Yin

Graduate School of Information Science and Technology, Hokkaido University, Sapporo, 060-0814, Japan

This paper extends the Dowell method and the semi-analytical homogenization method to analyze copper losses in a magnetic device in the time domain. The main contribution of this work is that the impedance provided by the Dowell method and the complex permeability resulting from the homogenization method are represented by the continued fractions and corresponding Cauer equivalent circuits, with which the time domain analysis can be effectively performed. The transient waveforms of the copper loss computed by the equivalent circuit in which the original leakage inductance is extended to a Cauer circuit are shown to be in good agreement with those computed by the finite element method. It is also shown that the Dowell method is valid only for the one-dimensional magnetic field over the winding region while the homogenization method is valid even when this assumption does not hold.

***Index Terms*—Dowell method, homogenization, complex permeability, Ollendorff formula, continued fraction, Cauer circuit.**

I. Introduction

IN RECENT years, the drive frequency of magnetic devices such as motors, reactors, and inductors has been increased in order to reduce their dimensions. As a result, the evaluation of eddy current losses in windings has become more critical. The finite element method (FEM) can accurately analyze eddy current losses in windings, although the computational cost increases when the number of windings becomes large. The situation becomes even more challenging when the skin depth is smaller than the winding radius. In such cases, the number of finite elements required to achieve sufficiently high accuracy is so large that the analysis may be impractical.

The Dowell method [1] and the homogenization method [2, 3] are known as effective methods for eddy current losses in windings, see, e.g., [4-8] for the former and [9-13] for the latter, respectively. The former method assumes that the permeability of the magnetic core is sufficiently high and that the magnetic field over the winding region varies in one dimension. This leads to an analytical expression for the impedance of multiple windings. Consequently, this method is highly effective for theoretical calculations of eddy current losses and is widely used in the design of magnetic devices, such as electric motors and power electronic circuits [4,5]. On the other hand, if the magnetic field over the winding region is not one-dimensional, as in an inductor, the Dowell method would no longer be valid. The validity of the Dowell method should also be carefully considered when the skin depth is less than the winding radius.

In the homogenization method, the eddy current loss and the effect of the antimagnetic field due to eddy currents in windings are expressed in terms of complex permeability, allowing the winding region to be replaced by a homogeneous material with complex permeability. This enables highly accurate eddy current analysis with coarse element partitioning that ignores the original structure of the winding. In particular, the semi-analytical homogenization based on the closed-form complex permeability does not require a preliminary FE analysis to obtain the complex permeability. In principle, this method is valid for the magnetic field that is not uniform in the coil region. If the above assumption of a one-dimensional magnetic field is valid, an analytical expression for the winding impedance can be derived and used for theoretical calculations as in the Dowell method.

Time domain analysis is necessary to determine the transient response of magnetic devices and the eddy current losses for distorted waves. Since the Dowell and the homogenization methods are formulated in the frequency domain, an extension to the time domain is necessary for application to such an analysis. However, to the authors' knowledge, there is no report that directly extends the Dowell and semi-analytical homogenization methods to the time domain. Sabariego et al. computed the impedance and complex permeability in the frequency domain using the numerical homogenization method. Then, the matrix entities in the time-domain circuit equations were determined by fitting so that they are consistent with the complex permeability obtained in the frequency domain [13]. Hiruma et al. obtained the complex permeability by the cell method using the numerical homogenization method and applied the Cauer via Lanczos (CVL) method based on the Lanczos algorithm to it to obtain a continued fractional representation [14]. The Cauer equivalent circuit derived from the continued fractions was then used for the time domain analysis. Moreover, Sato et al. performed a time-domain analysis by numerically evaluating the convolution integral that includes the inverse Laplace transform of the partial fractional expansion of the closed-form complex permeability [15]. Although the aforementioned methods have a wide range of applications, they require intricate numerical analysis, including fitting, CVL methods, and numerical inverse Laplace transforms.

Manuscript received April 1, 2015; revised May 15, 2015 and June 1, 2015; accepted July 1, 2015. Date of publication July 10, 2015; date of current version July 31, 2015.. Corresponding author: H. Igarashi (e-mail: igarashi.hokudai@gmail.com).

Digital Object Identifier (inserted by IEEE).

0018-9464 © 2015 IEEE. Personal use is permitted, but republication/redistribution requires IEEE permission.
See http://www.ieee.org/publications_standards/publications/rights/index.html for more information. (Inserted by IEEE.)

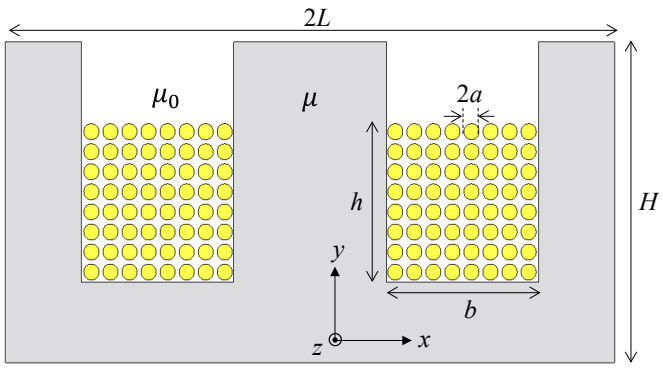


Fig.1 E-shaped magnetic core with multi-turn coil: $n_x = n_y = 8$, $a = 0.5$, $b = h = 10$, $H = 20$, $L = 20$, Depth=20 (unit:mm), $\mu = 1000\mu_0$, $\eta = 0.50, \eta' = 0.71$

This paper presents a unified and direct extension of the Dowell and semi-analytical homogenization methods for the time domain analysis. The proposed method derives the corresponding Cauer equivalent circuits through continued fractional expansion of the impedance or complex permeability given by the above methods in the frequency domain. The derived Cauer circuit can be included in the SPICE or other circuit simulator model for coupling analysis with other drive circuits. The proposed homogenization method can be considered as a model order reduction technique [9], which reduces a large system of equations to a small one. In addition, this paper compares the Dowell method with the semi-analytical homogenization method to clarify their accuracy and limitations of adaptability.

This paper is organized as follows. The next section formulates the Dowell and the semi-analytical homogenization methods in frequency domain. In Section 3, which is the main part of this paper, they are extended to the time domain through the continued fraction expansion and synthesis of the Cauer equivalent circuits. Section 4 numerically verifies accuracy of the semi-analytical homogenization and Dowell methods in the frequency domain to highlight their limitations. The accuracy of these methods in the time domain is then verified by comparing the transient responses computed by them with those obtained by direct application of the FEM to magnetic devices with windings discretized into sufficiently small elements.

II. Formulations in Frequency Domain

A. Dowell method

Let us consider an E-shaped magnetic core and a winding of radius a through which an alternating current flows, as shown in Figure 1. The magnetic permeability of the magnetic core is assumed to be sufficiently high, and the magnetic flux is assumed to have only a component in the x direction and to enter perpendicular to the magnetic core. Antiparallel eddy currents in the z direction flow in the cross section of each coil to counteract the time variation of magnetic flux. The model in Figure 1 is a simplified version of a motor stator, whereas the following arguments would also apply to transformers and inductors with one-dimensional magnetic fields over the winding. The coil radius $a = 0.5$ mm, which is a typical for motors [5], corresponds to the skin depth at about 20kHz and the core size was set sufficiently larger than a. To analyze this system, the multi-turn coil is considered as a foil conductor with a rectangular cross section that is long in the x direction.

By analyzing the electromagnetic induction and voltage drop in the conductors under this approximation, Dowell derived the impedance and AC resistance per unit length of each conductor given by [1]

$$Z_{ac} = R_{dc}\left\{\zeta\coth(\zeta) + \frac{2}{3}\left(n_y^2 - 1\right)\zeta\tanh\left(\frac{\zeta}{2}\right)\right\}, \tag{1a}$$

$$R_{ac} = \mathrm{Re}(Z_{ac}), \tag{1b}$$

where $\zeta = \alpha d, \alpha = (1+\mathrm{j})\sqrt{\eta'}/\delta, d = \sqrt{\pi}a$, $R_{dc} = 1/(\sigma d^2)$, $\delta = \sqrt{2/\mu_0\omega\sigma}$, and $\mathrm{j}, \sigma, \mu_0, \omega$ are imaginary unit, electric conductivity of the coil and permeability of vacuum, angular frequency and η' denotes the one-dimensional filling factor of the conductor. The first and second terms of (1a) represent the skin and proximity effects, respectively. The impedance of the multi-turn coil of length l, with n_x, n_y turns in x and y directions is given by $n_x n_y l Z_{ac}$ and $\eta' = \sqrt{\pi} n_x\, a/b$. If frequency is sufficiently low, (1a) reduces to

$$Z_{ac} \approx R_{dc} + j\omega\frac{1}{3}\left(n_y^2 - 1\right)\mu_0\eta', \tag{2}$$

where the first and second terms in (2) represent DC resistance and leakage inductance of the coil, respectively. The second term increases with n_y^2 because the magnetic induction B increases with n_y and the magnetic energy is proportional to B^2. There are different but equivalent expressions of R_{ac}, which are summarized in Appendix A.

B. Semi-analytical homogenization method

There are two approaches for homogenizing a winding: a numerical approach that computes the complex permeability by assuming a periodic structure and performing eddy current analysis of a unit cell of the periodic structure using a field computation method such as FEM; and a semi-analytical method that derives the closed-form homogenized complex permeability. In this study, we focus on the latter method, which is simpler and allows for physical interpretation.

Let us consider a round conductor of electric conductivity σ and relative magnetic permeability μ_r (where $\mu_r \approx 1$ for cupper) immersed in a time-harmonic uniform magnetic induction $B_0 e^{j\omega t}$. Antiparallel eddy currents are generated in the conductor to impede the time variation of the magnetic flux, thereby generating an antimagnetic field. This effect can be expressed by replacing the permeability of the conductor with the complex permeability given by [3,9]

$$\dot{\mu}_r = \mu_r\frac{J_1(z)}{zJ_1{}'(z)} = \mu_r\frac{1}{zJ_0(z)/J_1(z) - 1}, \tag{3}$$

where $z = a\sqrt{-j\omega\sigma\mu_0\mu_r} = (1-j)a/\delta$, and δ, J_n denote the skin depth and n-th order Bessel function, respectively, and prime denotes derivative. The real part of (3) represents the permeability considering the antimagnetic field due to eddy currents while the imaginary part is relevant to the effect of eddy current losses. By applying (3) to each conductor, the effect of eddy currents can be taken into account without the need for a fine finite element discretization to take skin depth into account. The eddy current loss density in the conductor can be obtained from (3) as follows [3,9]:

$$p = \frac{B_0^2}{2\mu_0}\mathrm{Re}\left(\frac{j\omega}{\dot{\mu}_r^*}\right) \quad [\mathrm{W/m^3}] \tag{4}$$

where * denotes complex conjugate. Eq. (4) is approximated by

$$p \approx \frac{1}{8}(B_0\omega a)^2\sigma \quad [\mathrm{W/m^3}] \tag{5}$$

if the frequency is sufficiently low, which is called the classical eddy current loss (Eq.(5) can be derived by using (14) to be given in III.B in (4)).

Next, we consider replacing the coil region shown in Figure 1 with a homogeneous material with equivalent electromagnetic property. By homogenization, eddy current analysis can be performed with coarse element partitioning of the homogeneous material instead of fine FE discretization that takes the coil structure into account. A magnetic dipole in a strand is generated by an external magnetic field and the sum of the magnetic fields generated by the dipoles acts on the strand as an external magnetic field. The homogenized permeability has to be determined so that they are consistent. In the case of a static magnetic field, the homogenized permeability is given by the Ollendorff formula [16, 3] given by

$$\langle\mu_r\rangle = 1 + \frac{\eta(\mu_r - 1)}{1 + N(1-\eta)(\mu_r - 1)}, \tag{6}$$

where N denotes the diamagnetic constant, where $N = 1/2$ for a round conductor, and η is the filling factor (volume fraction) which is given by $\eta = \pi a^2 n_x n_y/hb$ for the coil shown in Fig.1. Note here that η' for the Dowell method is different from η. The homogenized complex permeability of the multiturn coil, which takes into account the antiparallel eddy current due to the proximity effect that generates magnetic dipoles in a strand, can be obtained by inserting (3) to (6) as follows [3,9]:

$$\langle\dot{\mu}_r\rangle = 1 + \frac{2\eta\left\{\mu_r\frac{J_1(z)}{zJ_1'(z)} - 1\right\}}{2 + (1-\eta)\left\{\mu_r\frac{J_1(z)}{zJ_1'(z)} - 1\right\}}. \tag{7}$$

It is possible to perform eddy current analysis using magnetostatic FEM by simply using the homogenized complex permeability (7) in the winding region without fine discretization. The skin effect can be considered by using the AC resistance given by [9]

$$R_{ac} = R_{dc}\,\mathrm{Re}\left\{\frac{zJ_0(z)}{2J_1(z)}\right\}. \tag{8}$$

The different but equivalent expressions of (8) are summarized in Appendix B.

III. Formulations in Time Domain

Shindo et al. derived the complex permeability of an electromagnetic steel sheet using continued fractions [17]. Since the input impedance of a Cauer circuit (ladder circuit) can be expressed in terms of continued fractions, the Cauer circuit representation of the electromagnetic steel sheet can be obtained immediately. We will use a similar approach as above to extend the Dowell method and semi-analytical homogenization methods to the time domain.

A. Dowell method

We denote the first and second terms of (1a) representing the skin and proximity effects by Z_{skin} and Z_{prox}, respectively. Now, we apply the continued fraction expansion [18]

$$\tanh z = \frac{z}{1+}\frac{z^2}{3+}\frac{z^2}{5+}\frac{z^2}{7+}\cdots, \tag{9}$$

to Z_{skin} to obtain

$$\begin{aligned} Z_{skin} &= R_{dc}\left(1 + \frac{\zeta^2}{3+}\frac{\zeta^2}{5+}\frac{\zeta^2}{7+}\frac{\zeta^2}{9+}\cdots\right) \\ &= R_0 + \frac{1}{1/\mathrm{j}\omega L_1 +}\frac{1}{R_1 +}\frac{1}{1/\mathrm{j}\omega L_2 +}\frac{1}{R_2 +}\cdots, \end{aligned} \tag{10}$$

where $R_{dc}\zeta^2 = \mathrm{j}\omega\mu_0\eta'$. The inductance and resistance included in (10) are given by

$$L_n = \frac{\eta'\mu_0}{4n-1}, \qquad n = 1,2,\ldots, \tag{11a}$$

$$R_n = (4n+1)R_{dc}, \qquad n = 0,1,2,\ldots \tag{11b}$$

Similarly, Z_{prox} can be represented by

$$\begin{aligned} Z_{prox} &= qR_{dc}\frac{\zeta^2/2}{1+}\frac{(\zeta/2)^2}{3+}\frac{(\zeta/2)^2}{5+}\frac{(\zeta/2)^2}{7+}\cdots \\ &= \frac{1}{1/\mathrm{j}\omega L_1 +}\frac{1}{R_1 +}\frac{1}{1/\mathrm{j}\omega L_2 +}\frac{1}{R_2 +}\cdots, \end{aligned} \tag{12}$$

where $q = 2(n_y^2 - 1)/3$ and

$$L_n = \frac{\eta'\mu_0 q}{2(4n-3)}, \qquad n = 1,2,\ldots \tag{13a}$$

$$R_n = 2(4n-1)qR_{dc}, \qquad n = 1,2,\ldots \tag{13b}$$

Figure 2 shows the Cauer equivalent circuit corresponding to the continued fractions. Note here that the factor $2n_x n_y l$ is multiplied to (10) and (12) to obtain the input impedance of the winding shown in Fig.1. By evaluating the Joule loss from $p = \sum_k R_k i_k^2$ from the Cauer circuit, the eddy current loss for the

currents composed of harmonics in steady state and transient currents can be easily obtained. Figure 3 plots the AC resistance due to the proximity effect for the E-core model shown in Fig.1, normalized by R_{dc} of the winding, computed from Z_{prox} in (1) and the Cauer equivalent circuit constructed from (12). The abscissa is the winding radius normalized by the skin depth δ. It can be seen that the three-stage Cauer circuit is sufficiently accurate when $a/\delta \leq 4$. The expression of the skin effect (10) was found to have the similar tendency.

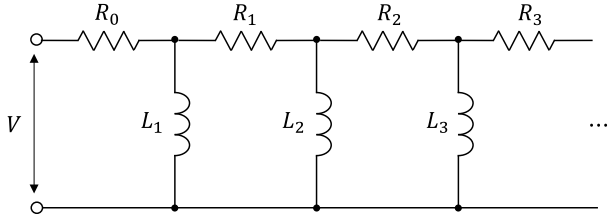


Fig.2 Cauer equivalent circuit for Dowell method (10) and (12)

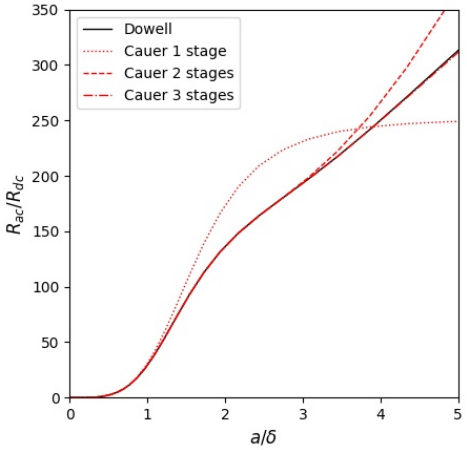


Fig.3 Comparison of Dowell formula (1) and corresponding Cauer circuits generated from (12) where $R_0 = 0$ and $\eta' = 0.71, n_y = 8$.

B. Semi-analytical Homogenization method

We apply the continued fraction expansion [18]

$$\frac{J_n(z)}{J_{n-1}(z)} = \frac{z}{2n-}\frac{z^2}{2(n+1)-}\frac{z^2}{2(n+2)-}\frac{z^2}{2(n+3)-}\cdots \tag{14}$$

to (7) and (3) to obtain

$$\begin{aligned} \mathrm{j}\omega\langle\dot{\mu}\rangle &= \frac{\mathrm{j}\omega\mu_0}{1+\eta}\left(1-\eta+\frac{4\eta}{-2\eta+(1+\eta)\dfrac{zJ_0(z)}{J_1(z)}}\right) \\ &= \frac{\mathrm{j}\omega\mu_0}{1+\eta}\left(1-\eta+\frac{4\eta}{2-\dfrac{z^2(1+\eta)}{4-}\dfrac{z^2}{6-}\dfrac{z^2}{8-}\cdots}\right) \\ &= \mathrm{j}\omega L_0+\frac{1}{1/\mathrm{j}\omega L_1+R_1+}\frac{1}{1/\mathrm{j}\omega L_2+R_2+}\frac{1}{}\cdots, \end{aligned} \tag{15}$$

where $\mu_r = 1$ is assumed for simplicity. The circuit parameters included in (15) are given by

$$L_0 = \frac{1-\eta}{1+\eta}\mu_0\,, \qquad L_1 = \frac{2\eta\mu_0}{1+\eta}\,, \tag{16a}$$

$$L_n = \frac{2\eta\mu_0}{(1+\eta)^2(2n-1)}\,, \qquad n = 2,3,\ldots \tag{16b}$$

$$R_n = \frac{16n\eta}{(1+\eta)^2\sigma a^2}, \qquad n = 1,2,\ldots \tag{16c}$$

Figure 4 shows the Cauer equivalent circuit corresponding to (15). Figure 5 plots the real and imaginary parts of $j\omega\langle\dot{\mu}\rangle$ computed from (7) and (15) for the E-core model shown in Fig.1, which are normalized by R_{dc}. It is found again that the three-stage Cauer circuit is sufficiently accurate when $a/\delta \leq 4$. Note that the continued fraction representation of the AC resistance (8) due to the skin effect can be found in [9, 17].

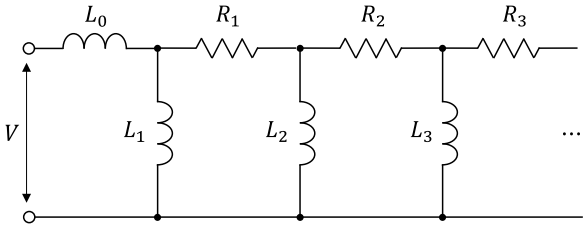


Fig.4 Cauer equivalent circuit for homogenization method (15)

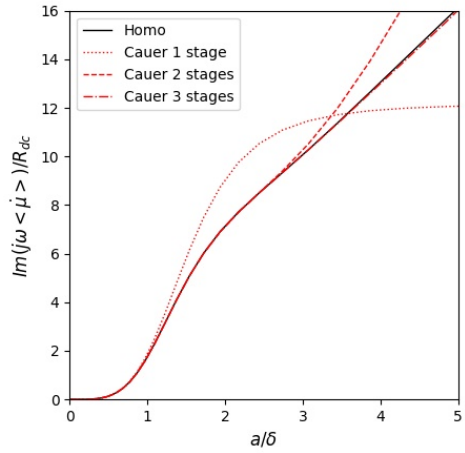


Fig.5 Comparison of homogenized complex permeability (7) and corresponding Cauer circuits generated from (15): $\eta = 0.50$

IV. Numerical Results

A. *Accuracy of homogenization method in frequency domain*

We first verify the accuracy of the semi-analytical homogenization method based on the macroscopic complex permeability (7) by comparing it with that computed by the numerical homogenization method in which the complex permeability is computed based on the FE analysis of the magnetic fields over the unit cell region Ω as follows:

$$\langle\dot{\mu}_r\rangle = \frac{\mathrm{j}\omega|\Omega||\boldsymbol{B}_0|^2}{\int_\Omega\left(\dfrac{\mathrm{j}\omega|\boldsymbol{B}|^2}{\mu_r}-\mu_0\sigma|\boldsymbol{E}|^2\right)dS}, \tag{17}$$

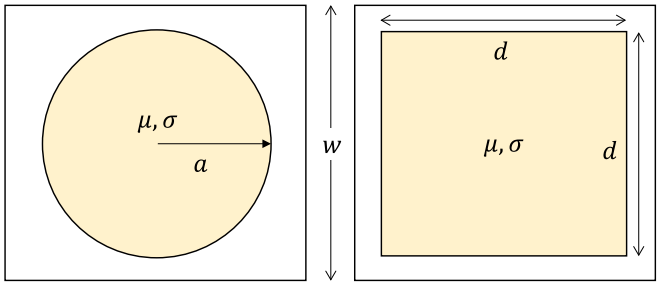


Fig.6 Unit cell models for round (left) and square (right) conductors

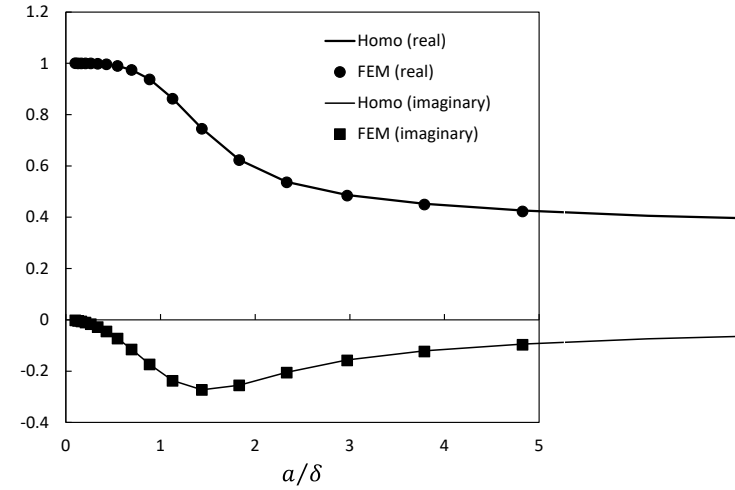
where $|\Omega|$, $\boldsymbol{B}_0$ denote the area of Ω, applied uniform magnetic induction and $\boldsymbol{B}$, $\boldsymbol{E}$ are the magnetic induction and electric field obtained by the magneto-quasistatic FE analysis. Note that (17) gives accurate values for arbitrary shaped conductors with sufficiently fine FE discretization. Figure 7 plots the frequency characteristics of $\langle\dot{\mu}_r\rangle$ computed by (7) and (17) for the round and squared shaped conductors shown in Fig.6. In addition to the case of the round conductor, the result from (7) is in good agreement with the result from (17) for the square conductor. This implies that the homogenization based on (7) gives accurate results not only for the round but also for the square conductors. The validity of FE analysis with (7) has also been shown by experiments [19-21].

On the other hand, it has been pointed out that (7) produces non-negligible errors when round conductors are arranged in the tightest packing with large filling ratio greater than, say, 0.8 rather than in a lattice arrangement as in Fig.1, [22]. Similarly, the error in (7) increases as the permeability of the conductor is increased. This is thought to be due to the fact that the derivation of (7) assumes a conductor in a uniform magnetic field, whereas the magnetic flux becomes non-uniform in the above situations. In fact, even with a filling factor of 0.9 for a square conductor, (7) has good accuracy, as shown in Fig. 7(b), probably due to the absence of flux concentration. Moreover, the accuracy of (7) hardly deteriorates even if the relative permeability is increased to 1000 for a square conductor. Therefore, to improve the accuracy of analytical homogenization (7), it may be necessary to take into account the non-uniformity of the magnetic flux, such as the flux concentration at the gaps. It has been shown that correcting for η can improve the accuracy in the case of high filling ratios [22].

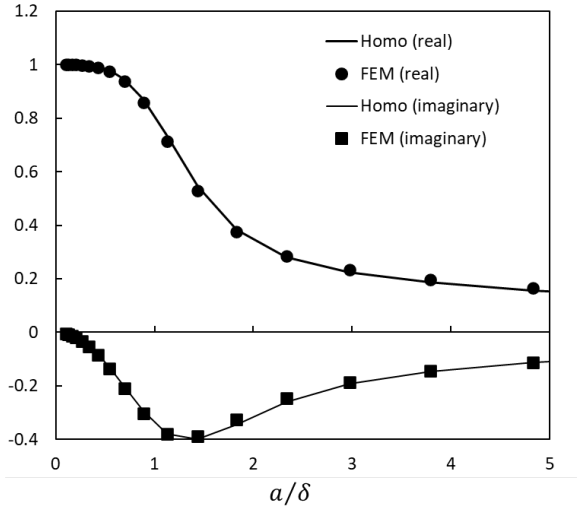
B. Comparison of Dowell and homogenization methods in frequency domain

To compare the Dowell method with the semi-analytical homogenization method in the frequency domain, they were applied to the E-core model shown in Fig.1 to compute the values of the AC resistance of the winding. It is assumed that $n_x = n_y = 8$. For the former, we computed $n_x n_y R_{ac}$ from (1), while for the latter, we evaluated it from the real part of

$$Z_{ac} = n_x n_y R_{dc} \frac{zJ_0(z)}{2J_1(z)} + \mathrm{j}\omega \frac{\langle\dot{\mu}\rangle}{I^2} \int_\Omega |\boldsymbol{H}|^2 dS. \tag{18}$$



(a) round conductor $\eta = 0.7$



(b)square conductor $\eta = 0.9$

Fig.7 Complex permeabilities computed by homogenization (7) and unit cell method (17) with FEM

where Ω denotes the coil region, and the magnetic field was computed by the magnetostatic FEM and $\langle\dot{\mu}\rangle$ is computed from (7). As the most accurate method, a magneto-quasistatic FE analysis was performed by dividing the multi-turn coil into elements that are sufficiently finer than the skin depth. The frequency characteristics of the AC resistance obtained by these three methods are plotted in Fig.8. When the relative permeability of the magnetic core is 1000 and $\delta > a$, the three are in good agreement. However, when the frequency increases and the condition $\delta > a$ is not satisfied, accuracy of the Dowell method slightly deteriorates. When the relative permeability of the magnetic core is 30 (corresponding to a magnetic powder core), the Dowell method which assumes infinite permeability loses its validity as expected. On the other hand, the results of the homogenization method using (7) are in good agreement with those computed by FEM, regardless of the conditions of frequency and permeability. Figure 9 shows the magnetic flux distribution obtained by the conventional FEM, where the coil is divided into finite elements sufficiently smaller than δ, and that obtained by the homogenized FEM, in which the conductor

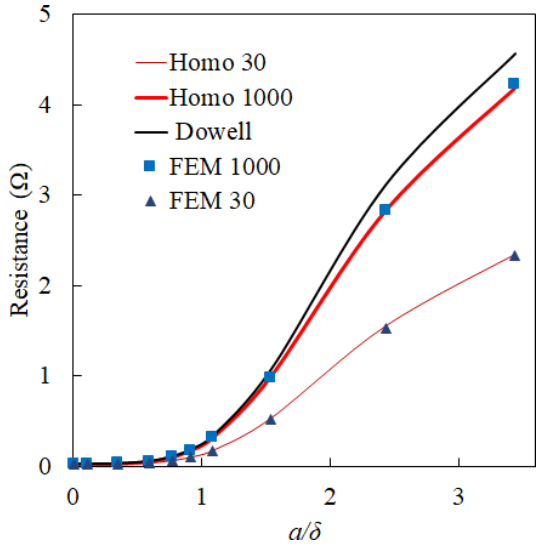


Fig.8 Comparison of AC resistances computed by Dowell method (1), homogenization (7) and FEM with fine discretization. Numbers are relative permeability of the core.

region is represented by a homogeneous material with the permeability given by (7), which is divided into coarse elements. They are in good agreement.

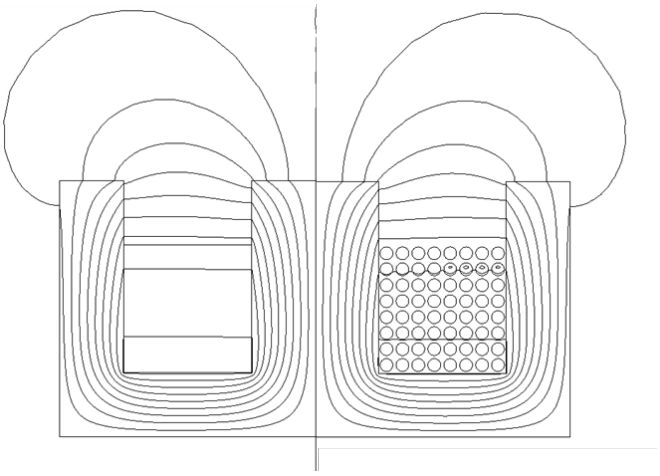


Fig.9 Magnetic flux lines computed by homogenized FEM (left) with (7) and conventional FEM with fine mesh (right) at 100kHz ($a/\delta = 2.44$). The field over the coil is almost one-dimensional.

The evaluation using (18) requires an FE analysis. The semi-analytical homogenization method was compared with the Dowell method in frequency domain under the assumption that the magnetic permeability of the magnetic core is sufficiently high and that the magnetic field is one-dimensional as in the Dowell method in [23, 24]. Using this approach assuming that $H_x = n_x n_y I\, y/hb$ in (18), the analytical expression of Z_{ac} can be obtained as follows:

$$Z_{ac} = n_x n_y R_{dc} \frac{zJ_0(z)}{2J_1(z)} + \frac{j\omega}{3b} h\left(n_x n_y\right)^2 \langle \dot{\mu} \rangle \ . \qquad (19)$$

When the magnetic permeability of the magnetic core is sufficiently high, Z_{ac} obtained from (19) agrees well with that from (18), the latter of which is based on FEM. The AC resistance computed from (19) and (1) is plotted in Fig. 10 for different values of n_y. It is interesting that they give results that agree rather well, although the mathematical expressions of the two are quite different. When $a/\delta > 1$, they can differ by about 5%. It was also found that the difference tends to decrease as the number of turns n_x increases. This is a point to keep in mind when using these approaches.

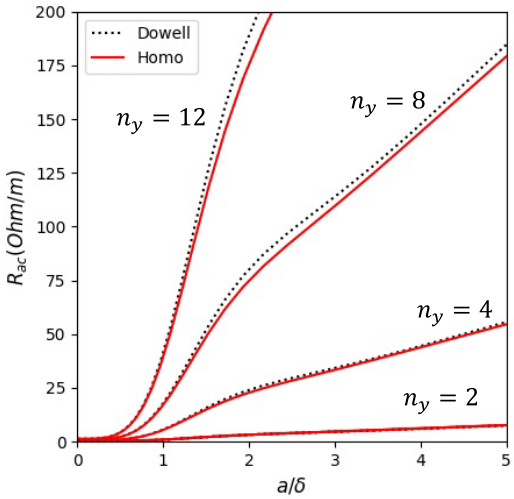


Fig. 10 Comparison of R_{ac} computed from Dowell method (1) and homogenization (19) ($n_x = 8$)

C. Comparison of Dowell and homogenization methods in time domain

We now apply the Cauer equivalent circuits obtained from (12) for the Dowell method and (15) for the semi-analytical homogenization method to the time-domain analysis of the E-core model shown in Fig.1. Since the skin effect is much smaller than the proximity effect, the former was neglected. Moreover, the magnetic field was analytically represented as in (19) for the homogenization method since the magnetic field over the coil region can be assumed to be one-dimensional for this model. Table I summarizes the circuit parameters, which are computed from (12) and (13) for the Dowell method, and (15), (16) and the second term of (19) for the homogenization method. Figure 11 shows the equivalent circuit where $L_0 + L_1$ represents the leakage inductance without the effect from eddy currents, and L_0 is set to zero for the Dowell method. Moreover, R_0 and L_{core} are the DC resistance of the coil and primal inductance of the core, respectively, the latter being obtained by subtracting $L_0 + L_1$ from the total inductance obtained from the magnetostatic FE analysis. We also performed the transient FE analysis with sufficiently small discretization. Figure 12 shows the time evolution of the Joule loss, where "Dowell DC" is the loss due to DC resistance and "Dowell total" is the total loss including the eddy current loss. In this case, where $a \approx \delta$ for the fundamental frequency, the eddy current loss is significant due to the proximity effect. The temporal evolution of the eddy current loss computed from the equivalent Cauer circuits for the Dowell and homogenization

methods are in good agreement with that computed by the transient FEM, where the maximum difference to FEM is about 5mW. It is emphasized that it is sufficient to simply extend the leakage inductance in the conventional equivalent circuit of electrical machines to a Cauer circuit to account for the eddy current loss in the winding.

If the magnetic permeability of the magnetic material is relatively low and the magnetic field does not vary in one dimension, time-domain analysis based on the Dowell method (12) or the analytical homogenization method (15) and (19) would not be effective. Is the semi-analytical homogenization method (15) and (18) effective for such an analysis? To answer to this question, we constructed the Cauer circuit based on (15) and (18) for the inductor model with magnetic core of $\mu_r = 30$ shown in Fig.13, which would correspond to the soft magnetic composite. Since the magnetic field does not have one-dimensional distribution in the coil region, we computed the magnetic field using the magnetostatic FEM to evaluate the integral of $|\boldsymbol{H}|^2$ in (18), which was found to have little dependence on frequency when it is less than 10kHz. Table II summarizes the circuit parameters in the Cauer circuit, which are computed from (15), (16) and the second term of (18). The result of this method was compared with that computed by the transient FEM with sufficiently fine discretization. They are in good agreement as shown in Fig.14, where the maximum difference is about 0.21mW. It is, therefore, expected that the homogenization method based on (15) and (18) can be applied to wide class of problems where the assumption that the magnetic field is one-dimensional over the winding does not hold while the Dowell method based on (12) and the fully analytical homogenization based on (15) and (19) are accurate under the one-dimensionality assumption and easy to use due to their simplicity.

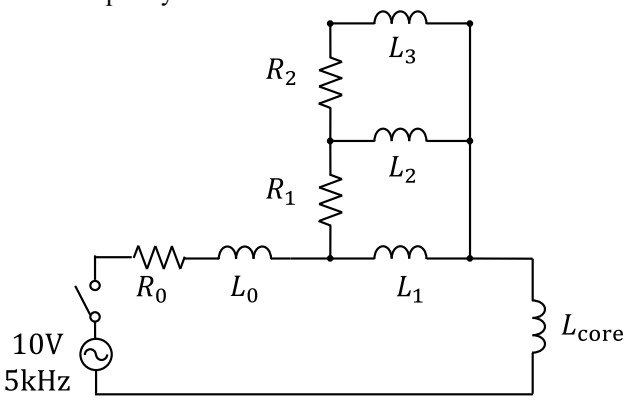


Fig. 11 Cauer circuit for time-domain analysis of E-core model shown in Fig.1. The switch is ON at $t = 0$.

Table I Circuit parameters for E-core model shown in Fig.1 (Unit: Ω, μH)

	R_0	R_1	R_2	L_0	L_1	L_2	L_3	L_{core}
Dowell	2.1 $\times 10^{-2}$	13	32	0	48	9.6	5.3	249
Homo	2.1 $\times 10^{-2}$	14	26	23	46	10	6.1	228

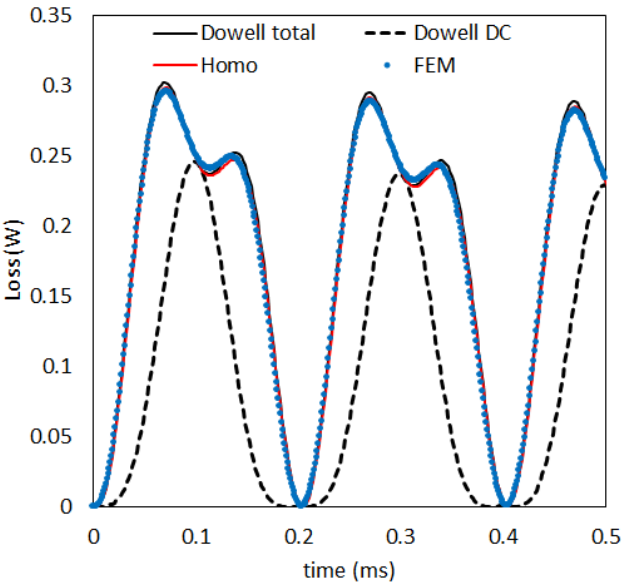


Fig. 12 Time-variation of eddy current losses of E-core model shown in Fig.1

D. Use of semi-analytical homogenization method

We summarize here the use of the semi-analytical homogenization method for time-domain analysis. In this method, the circuit parameters for the Cauer circuit representing the complex permeability $\langle\dot{\mu}\rangle$ shown in Fig.4 are analytically evaluated from (16).

We have paid attention to the method in which the input impedance Z_{ac} of a magnetic device is represented by an equivalent circuit including the Cauer circuit. For this method, the Cauer circuit for $\langle\dot{\mu}\rangle$ has to be converted to that for Z_{ac} through either (18) or (19). There are following two cases:

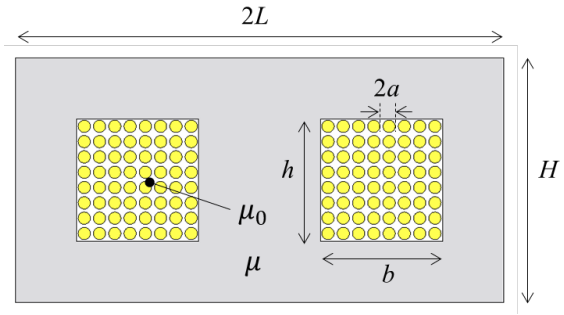
(i) When the magnetic field is one-dimensional over the coil region Ω, such as in the E core model shown in Fig.1, the circuit parameters for Z_{ac} are evaluated analytically by (19).

(ii) When the magnetic field is not one-dimensional over Ω, such as in the inductor model shown in Fig.13, the circuit parameters for Z_{ac} are obtained by (18), which involves numerical integration of the magnetic field over Ω.

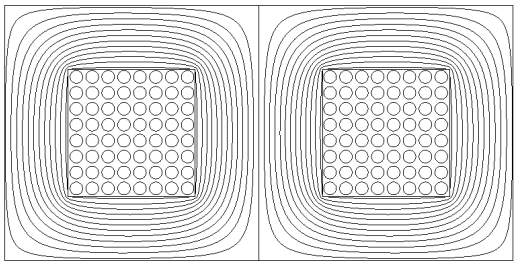
Note that the core inductance L_{core} is computed by magnetostatic FEM in both (a) and (b). There is still another way for the time-domain analysis based on this method, that is,

(iii) The Cauer circuit representing $\langle\dot{\mu}\rangle$ shown in Fig.4 is coupled with the FE equation as described in [23] which presents the numerical homogenization method.

In method (iii), the whole magnetic device is not modeled by the equivalent circuit as in Fig.11 using (i) or (ii), but is modeled by the FE equation coupled with circuit equations for coils. This method can deal with the problems where eddy currents exist in the region other than the coil region.



(a) Structure $L = H = 20, h = b = 10, a = 0.5,$ depth is 20 (unit:mm), $\mu = 30\mu_0, \eta = 0.50.$



(b) Magnetic flux lines computed by FEM

Fig. 13 Inductor model

Table II Circuit parameters for inductor model shown in Fig.13 (Unit: Ω, μH)

	R_0	R_1	R_2	L_0	L_1	L_2	L_3	L_{core}
Homo	5.4 $\times 10^{-2}$	2.1	4.3	3.8	7.6	1.7	1.0	640

V. Conclusions

This paper has extended the Dowell and semi-analytical homogenization method to the time domain. To this end, the impedance for the Dowell method and the complex permeability for the homogenization method are represented in the continued fractions, from which the Cauer equivalent circuits are synthesized, which are the main contributions of this work. It has been shown in the frequency domain that the AC resistance computed by the Dowell method agrees well with that obtained by the homogenization method under the condition that the magnetic core has a sufficiently high permeability so that the magnetic field over the coil region is one-dimensional. The transient Joule losses for the E-core model computed by the proposed equivalent circuits including the Cauer circuit have been shown to be in good agreement with those obtained by the FEM under the above condition. It has been shown that homogenization also yields the transient Joule loss for the inductor model with good accuracy, where the magnetic field is not one-dimensional but distributed over the coil region.

It has been shown that the effect of magnetic saturation in a magnetic core can be considered at high accuracy by introducing nonlinear BH characteristic to the primal inductor of the Cauer circuit [25]. This is expected to be the case for the Cauer circuits presented in this paper. This discussion remains for future work.

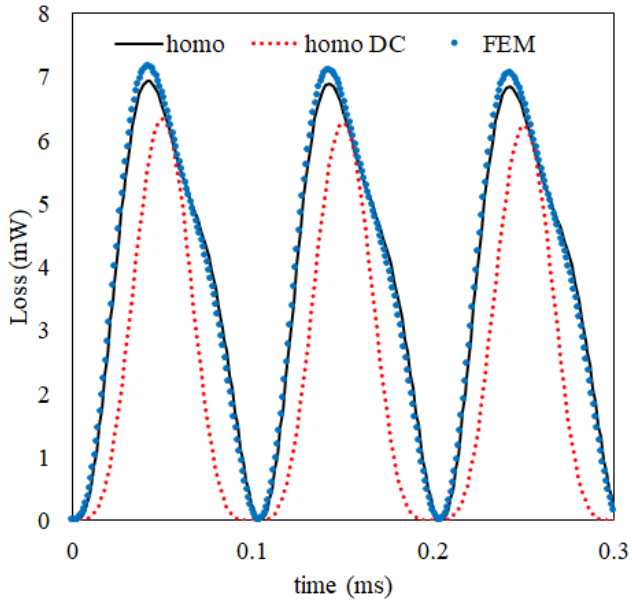


Fig. 14 Time-variation of eddy current losses of inductor model shown in Fig.13

Appendix A

Here we summarize different but equivalent expressions of R_{ac} resulted from the Dowell method. It can be shown by long but straightforward computations that Eq. (1) is expressed as

$$R_{ac} = R_{dc}\xi\left\{\mathcal{U}(\xi) + \tfrac{1}{3}(n_y^2 - 1)\mathcal{V}(\xi)\right\}, \tag{A1}$$

where $\xi = a\sqrt{\pi\eta'}/\delta$ and $\mathcal{U}, \mathcal{V}$ are defined by

$$\mathcal{U}(\xi) = \frac{\sinh 2\xi + \sin 2\xi}{\cosh 2\xi - \cos 2\xi}, \tag{A2}$$

$$\mathcal{V}(\xi) = 2\frac{\sinh \xi - \sin \xi}{\cosh \xi + \cos \xi}. \tag{A3}$$

On the other hand, Perry and Ferreria analyzed the eddy current loss in the foil conductor to derive the AC resistance of the n-th layer of the foil conductor given by [26, 27]

$$\begin{aligned} R_{ac}(n) &= R_{dc}\xi\{\mathcal{U}(\xi) + n(n-1)\mathcal{V}(\xi)\} \\ &= R_{dc}\xi\{(2n^2 - 2n + 1)\mathcal{U}(\xi) - 4n(n-1)\mathcal{W}(\xi)\}, \end{aligned} \tag{A4}$$

where

$$\begin{aligned} \mathcal{W}(\xi) &= \frac{1}{4}\{2\mathcal{U}(\xi) - \mathcal{V}(\xi)\} \\ &= \frac{\sinh \xi \cos \xi + \cosh \xi \sin \xi}{\cosh 2\xi - \cos 2\xi}. \end{aligned} \tag{A5}$$

We obtain the average AC resistance by substituting (A4) to

$$R_{ac} = \frac{1}{n_y}\sum_{n=1}^{n_y} R_{ac}(n), \tag{A6}$$

which leads to (A1).

APPENDIX B

The AC resistance R_{ac} of a round conductor due to skin effect is given by (8), which can be modified to have the following different expression which is presented in [27]:

$$R_{ac} = \frac{xR_{dc}}{2}\frac{\mathrm{ber}(x)\mathrm{bei}'(x) - \mathrm{bei}(x)\mathrm{ber}'(x)}{\left(\mathrm{ber}'(x)\right)^2 + \left(\mathrm{bei}'(x)\right)^2} \tag{B1}$$

where ber and bei are the Kelvin functions and $x = \sqrt{2}a/\delta$. If a round conductor is approximated by the square conductor of the same area, the following expression is also possible [27, 28]

$$R_{ac} \approx \frac{yR_{dc}}{2}\frac{\sinh y - \sin y}{\cosh y + \cos y} \tag{B2}$$

where $y = \sqrt{\pi}a/\delta$.

REFERENCES

[1] P. L. Dowell, Effects of eddy currents in transformer windings, Proc. Inst. Elect. Eng., vol. 113, no. 8, 1387–1394, 1966.

[2] J. Gyselinck, P. Dular, Frequency-domain homogenization of bundles of wires in 2-D magnetodynamic FE calculations, IEEE Trans. Magn., vol.41, no.5, pp.1416-1419, 2005.

[3] H. Igarashi, Semi-analytical approach for finite-element analysis of multi-turn coil considering skin and proximity effects, IEEE Trans. Magn., 53(1), 7400107, 2017.

[4] R.W. Erickson, D. Maksimović, Fundamentals of Power Electronics, Springer, 2020.

[5] J. Pyrhonen, T. Jokinen, V. Hrabovcova, Design of rotating electrical machines, John Wiley & Sons, 2013.

[6] X. Nan, C. R.Sullivan, An improved calculation of proximity-effect loss in high-frequency windings of round conductors. In IEEE 34th Annual Conference on Power Electronics Specialist, PESC'03. vol.2, 853-860, 2003.

[7] A. Reatti, M.K. Kazimierczuk, Comparison of various methods for calculating the AC resistance of inductors, IEEE Trans. Magn., 38(3), 1512-1518, 2002.

[8] A.D. Podoltsev, I.N. Kucheryavaya, B.B. Lebedev, Analysis of effective resistance and eddy-current losses in multiturn winding of high-frequency magnetic components, IEEE Trans. Magn., 39(1), 539-548, 2003.

[9] H. Igarashi, Topology optimization and AI-based design of power electronic and electric devices, Academic Press, 2024.

[10] G. Volpe, M. Popescu, F. Marignetti, J. Goss, AC winding losses in automotive traction e-machines: A new hybrid calculation method, 2019 IEEE International Electric Machines & Drives Conference (IEMDC), 2115-2119, 2019.

[11] K. Niyomsatian, J.J. Gyselinck, R.V. Sabariego, Experimental extraction of winding resistance in litz-wire transformers—Influence of winding mutual resistance. IEEE Trans. Power Electronics, 34(7), 6736-6746, 2018.

[12] S. Gyimóthy, et al., Loss computation method for litz cables with emphasis on bundle-level skin effect. IEEE Trans. Magn., 55(6), 6300304, 2019.

[13] R. V. Sabariego, P. Dular, J. Gyselinck, Time-domain homogenization of windings in 3-D finite element models, IEEE Trans. Magn., vol.44, no.6, pp.1302-1305, 2008.

[14] S. Hiruma, H. Igarashi, Time-domain analysis of homogenized finite-element method for eddy current analysis with reduced unknown variables, IEEE Trans. Magn., 56(1), 7501604, 2020.

[15] Y. Sato, S. Hiruma, H. Matsumoto, H. Igarashi, Time-domain homogenized finite eddy current analysis using recursive convolution method, IEEE Trans. Magn. 59(5), 7400904, 2023.

[16] F. Ollendorff, Magnetostatik der massekerne, Arch. Elektrotechnik, vol.25, no.6, pp. 436–447, 1931.

[17] Y. Shindo, O. Noro, Simple circuit simulation models for eddy current in magnetic sheets and wires, IEEJ Trans. A, 134(4), 173-181, 2014.

[18] M. Abramowitz, , I. A. Stegun, Eds., Handbook of mathematical functions with formulas, graphs, and mathematical tables, Vol. 55, Dover, 1948.

[19] X. Xu, Z.Xu, Modeling and analysis of Litz wire radio frequency (RF) coil in inside-out NMR well logging sensor, IEEE Trans. Geoscience and Remote Sensing, 61, 2001209, 2023

[20] T. Chen, T. Zhao, Z. Shen, H. Jia, H. Wang, Litz-wire winding loss calculation method for optimal design of high-frequency transformers. IEEE J. Emerging and Selected Topics in Power Electronics, 12(2), pp.2027-2040, 2024.

[21] D.Y. Um, S. A. Chae, G.S. Park, AC-Winding-Resistance Calculation of Toroidal Inductors with Solid-Round-Wire and Litz-Wire Winding Based on Complex Permeability Modeling. Machines, 12(4), 228, 2024.

[22] K. Niyomsatian, J. Gyselinck, R.V. Sabariego, Closed-form complex permeability expression for proximity-effect homogenisation of litz-wire windings, IET Science, Measurement & Technology, 14(3), 287-291, 2020.

[23] S. Hiruma, H. Igarashi, Homogenization method based on Cauer circuit via unit cell approach, IEEE transactions on magnetics, 56(2), 7505805, 2020.

[24] S. Hiruma, Study on model order reduction for Maxwell's equations based on Krylov subspace methods, Dissertation, Hokkaido Univ., 2021.

[25] Y. Sato, T. Shimotani, H.Igarashi, Synthesis of Cauer-equivalent circuit based on model order reduction considering nonlinear magnetic property, IEEE Trans. Magnetics, 53(6), 1100204, 2017.

[26] M.P. Perry, Multiple layer series connected winding design for minimum losses, IEEE Trans. Power Appl. Syst. PAS-98, pp.116-123, 1979.

[27] J.A. Ferreira, Improved analytical modeling of conductive losses in magnetic components. IEEE Trans. Power Electronics, 9(1), pp.127-131, 1994.

[28] R.L. Stoll, The analysis of eddy currents, Oxford-Clarendon Press, 1974.

H. Igarashi (M'94-) received the Ph.D. degree in engineering from Hokkaido University in 1992. He has been a professor at Graduate School of Information Science and Technology, Hokkaido University, since 2004. He has worked as a research engineer at Canon Co. Ltd., from 1984 to 1989. From 1989 to 1999, he was a research associate with the Faculty of Engineering, Hokkaido University. He was a guest researcher at Berlin Technical University, Germany, under support from the Humboldt Foundation from 1995–1997. His research area is computational electromagnetism, optimal design and AI-based design of electric machines. He has authored and coauthored more than 300 peer-reviewed journal papers.

Q. Liu received the Ph.D. degree in engineering from Hokkaido University in 2024.

S. Yin received the Ph.D. degree in engineering from Politechnico di Milano in 2021. She is currently a postdoctoral fellow at Graduate School of Information Science and Technology, Hokkaido University.